

HNU-EBL: A Software Toolkit for Electron Beam Lithography Simulation and Optimization

1st Wei Liu

College of Electrical and Information
Engineering
Hunan University
Changsha, China
liuw@hnu.edu.cn

2nd Wenze Yao

College of Electrical and Information
Engineering
Hunan University
Changsha, China
wenzeyao@hnu.edu.cn

3rd Chengyang Hou

College of Electrical and Information
Engineering
Hunan University
Changsha, China
houchengyang@hnu.edu.cn

4th Hongcheng Xu

College of Electrical and Information
Engineering
Hunan University
Changsha, China
hongchengxu@hnu.edu.cn

5th Haojie Zhao

College of Electrical and Information
Engineering
Hunan University
Changsha, China
haojie_zhao@hnu.edu.cn

6th Yiqin Chen

College of Mechanical and Vehicles
Engineering
Hunan University
Changsha, China
chenyiqin@hnu.edu.cn

7th Huigao Duan

College of Mechanical and Vehicles
Engineering
Hunan University
Changsha, China
duanhg@hnu.edu.cn

8th Jie Liu

College of Electrical and Information
Engineering
Hunan University
Changsha, China
jie_liu@hnu.edu.cn

Abstract—This paper introduces a software toolkit, HNU-EBL, developed at Hunan University (HNU), to simulate and optimize electron beam lithography (EBL). The toolkit consists of three consecutive modules. Firstly, the electron trajectories in EBL resist and substrate layers are simulated by using Monte Carlo (MC), and point spread function (PSF) is obtained by fitting the electron trajectories. Secondly, using PSF, electron dose distribution is optimized using the fast Fourier transform (FFT), to efficiently correct the effects like proximity effect and fogging effect that may jeopardize the lithography resolution and pattern quality. Thirdly, based on the optimized electron dose distribution, the optimized pattern quality is evaluated based on metrics like the edge placement error (EPE). The HNU-EBL toolkit can simulate sub-10 nm EBL, and it has been successfully applied to optimize fabrication of nm-scale devices.

Keywords—electron beam lithography (EBL), Monte Carlo (MC), fast Fourier transform (FFT), point spread function (PSF), proximity effect correction (PEC), edge placement error (EPE).

I. INTRODUCTION

Electron beam lithography (EBL) is widely used in device and mask fabrications [1-3], due to its high lithography resolution and flexible mask-less direct-write characteristics. However, due to scattering of incident electrons, the EBL resist at one location $\mathbf{r} = (x, y)$ may suffer from significant undesirable exposure from electron beams incident at other locations $\mathbf{r}' = (x', y')$. These effects are referred to as EBL proximity effects (PE) and fogging effects (FE), which exert considerable negative impacts on the resolution and pattern fidelity of EBL [4-8].

It is desirable to perform calculations to correct PE and FE before EBL fabrication, in order to ensure fabrication quality and pattern fidelity. However, due to the high complexity of the electron scattering process and the huge number of pixels in the lithography pattern, those correction calculations are very sophisticated to program and computationally expensive to run [4].

In this paper, we briefly introduce a software toolkit (“HNU-EBL”) we developed at Hunan University (HNU), to perform those correction and optimization calculations. The EBL fabrication quality after electron dose correction can be quantitatively evaluated by using metrics like edge placement error (EPE) [9].

As schematically shown in the Fig. 1, the proposed HNU-EBL toolkit consists of seven parts: #1 electron scattering MC calculator, #2 electron trajectories calculator, and #3 PSF calculator belong to the first module, which is introduced in Section II; #4 energy deposition calculator and #5 incident electron dose correction calculator belong to the second module, which is discussed in Section III; #6 EPE calculator and #7 visualization of GDSII files belong to the third module, which is introduced in Section IV. A brief conclusion is made in Section V.

II. ELECTRON TRAJECTORY AND PSF CALCULATION

In the first module, HNU-EBL users are allowed to create different simulation projects for various EBL optimization tasks. In each task, after entering chemical compositions and mass densities of EBL resist and substrate, electron trajectories and PSF can be obtained by using the MC simulations [10, 11], as shown in Fig. 2. The double-Gaussian (2G) as shown in Equation (1), triple-Gaussian (3G) as shown in Equation (2), and triple-Gaussian plus single-exponential (3G+1E) as shown in Equation (3) can be used to approximate the electron beam energy deposition [8, 12, 13].

In Equations (1), (2), and (3), $r = |\mathbf{r} - \mathbf{r}'|$; α , β , and η are the coefficients representing the forward scattering range, back scattering range, and the relative strength between forward scattering and back scattering [14]; the term with γ and the term with γ_2 are the third Gaussian term and the exponential term, respectively, added to better approximate the PSF; η' and η'' are coefficients that define the magnitude of the added terms in PSF.

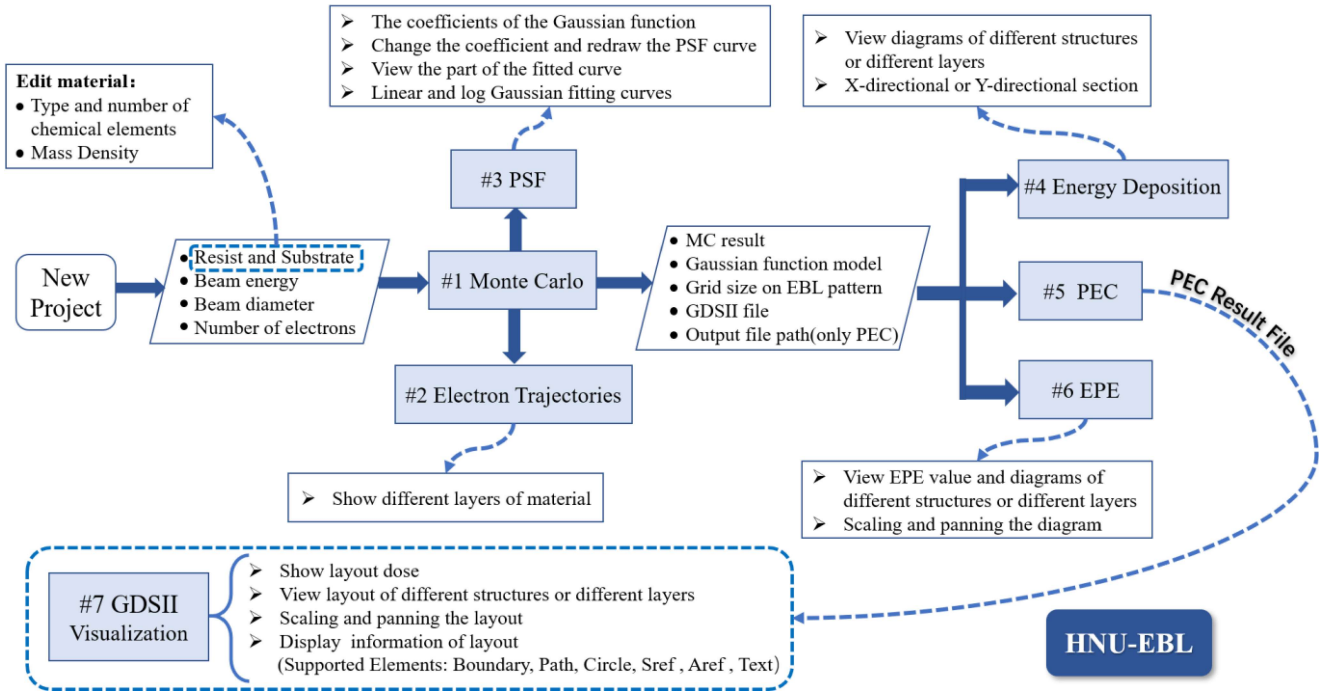


Fig. 1. Schematic flowchart of the HNU-EBL toolkit, which consists of seven parts. (1) Monte Carlo calculation; (2) Electron trajectories simulation; (3) Point spread function (PSF) calculation; (4) energy deposition calculation; (5) FFT-based incident electron dose correction calculation; (6) Edge placement error (EPE) calculation; and (7) GDSII file visualization.

$$P(\mathbf{r}, \mathbf{r}') = \frac{1}{\pi(1+\eta)} \left[\frac{1}{\alpha^2} \exp\left(-\frac{r^2}{\alpha^2}\right) + \frac{\eta}{\beta^2} \exp\left(-\frac{r'^2}{\beta^2}\right) \right] \quad (1)$$

$$P(\mathbf{r}, \mathbf{r}') = \frac{1}{\pi(1+\eta+\eta')} \left[\frac{1}{\alpha^2} \exp\left(-\frac{r^2}{\alpha^2}\right) + \frac{\eta}{\beta^2} \exp\left(-\frac{r'^2}{\beta^2}\right) + \frac{\eta'}{\gamma^2} \exp\left(-\frac{r'^2}{\gamma^2}\right) \right] \quad (2)$$

$$P(\mathbf{r}, \mathbf{r}') = \frac{1}{\pi(1+\eta+\eta'+\eta'')} \left[\frac{1}{\alpha^2} \exp\left(-\frac{r^2}{\alpha^2}\right) + \frac{\eta}{\beta^2} \exp\left(-\frac{r'^2}{\beta^2}\right) + \frac{\eta'}{\gamma^2} \exp\left(-\frac{r'^2}{\gamma^2}\right) + \frac{\eta''}{2\gamma_2^2} \exp\left(-\frac{r'^2}{\gamma_2^2}\right) \right] \quad (3)$$

In HNU-EBL toolkit, the users are allowed to choose any PSF, among 2G PSF as shown in Equation (1), 3G PSF as shown in Equation (2), and 3G+1E PSF as shown in Equation (3).

Then, the fitted PSF curves can be plotted against the electron trajectory data, using the graphics user interface (GUI) of HNU-EBL toolkit, as shown in Fig.2(b).

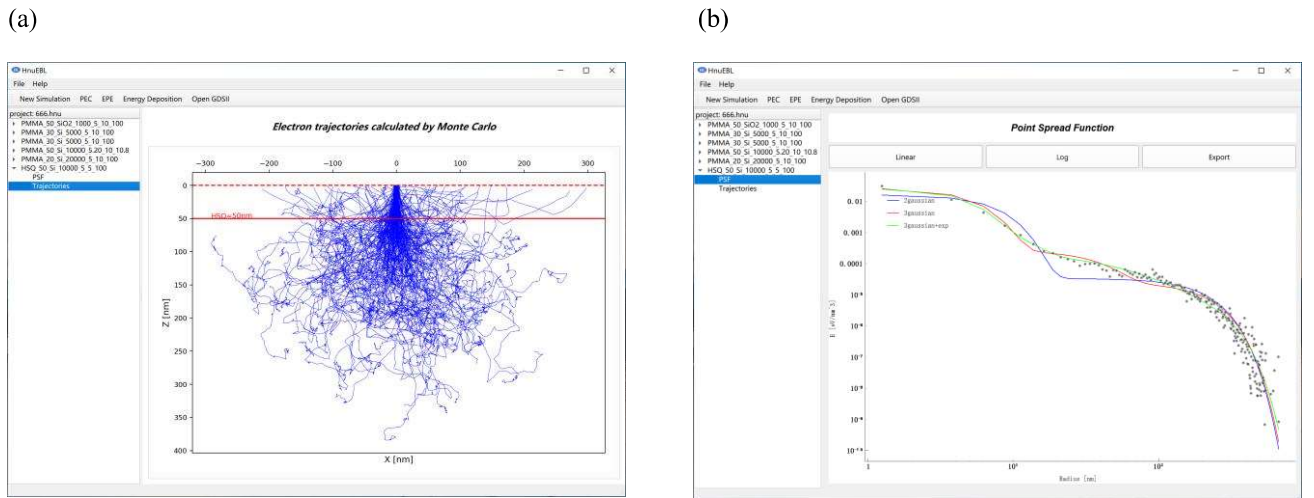


Fig. 2. The electron trajectories simulation results (a); and the point spread function (PSF) calculation results (b).

III. ENERGY DEPOSITION AND DOSE CORRECTION

It is known that the electron energy deposition is the convolution between the incident electron dose distribution and the PSF, as shown in Equation (4) [15]. Given a dose distribution $d(\mathbf{r})$, where $\mathbf{r} = (x, y)$, the energy deposition $E(\mathbf{r})$ is computed as

$$E(\mathbf{r}) = K \iint P(\mathbf{r}, \mathbf{r}') d(\mathbf{r}') d^2 \mathbf{r}' \quad (4)$$

where K is a constant; $P(\mathbf{r}, \mathbf{r}')$ is the PSF as shown in Equations (1), (2), and (3).

In the HNU-EBL toolkit, the user inputs parameters to start the energy deposition calculation (#4 in Fig.1). When the calculation is completed, the energy deposition is displayed on GUI (Fig.3(c, d)).

The FFT, whose calculation time complexity is $O(N \log(N))$, is used here to perform the convolution calculations as shown in Equation (4), where N is the number of pixels in the EBL [16]. Based on a structured (i.e., equally spaced) grid for discretization [17], the energy deposition is computed by using

$$E(x, y) = \mathcal{F}^{-1} [\mathcal{F} [P(x, y)] \mathcal{F} [D(x, y)]] \quad (5)$$

where $P(x, y)$, $D(x, y)$ and $E(x, y)$ are PSF, the target EBL fabrication pattern, and the energy deposition matrix with two-dimensional equally spaced matrix representation, respectively; operator $\mathcal{F}[\cdot]$ and $\mathcal{F}^{-1}[\cdot]$ are two-dimensional Fourier transform and inverse Fourier transform.

Adjusting exposure dose can change electron energy deposition to complete the PEC by 2D-FFT [17, 18]. As shown in the Fig.3(a, b), it is easy to view the dose of PEC result file using the GDSII file visualization module (#7 in Fig.1) after the PEC calculation is completed. From the Fig.3(c, d), it can be seen that PEC could effectively improve the resolution of EBL.

To test the performance of the HNU-EBL, we run a PEC calculation of an EBL pattern with a maximum of $N=10^8$ pixels, on a computer with Intel(R) Core (TM) i5 CPU (2.40 GHz) and 16G RAM. On the same machine, NanoPECS (an established commercial PEC software offered by Raith [13]). The same test layout is M gratings with a size of $1\mu\text{m} \times 50\text{nm}$ shown in Fig.4(a). As shown in the Fig.4(b), the calculation speed of HNU-EBL is an order of magnitude faster than NanoPECS under the same calculation accuracy.

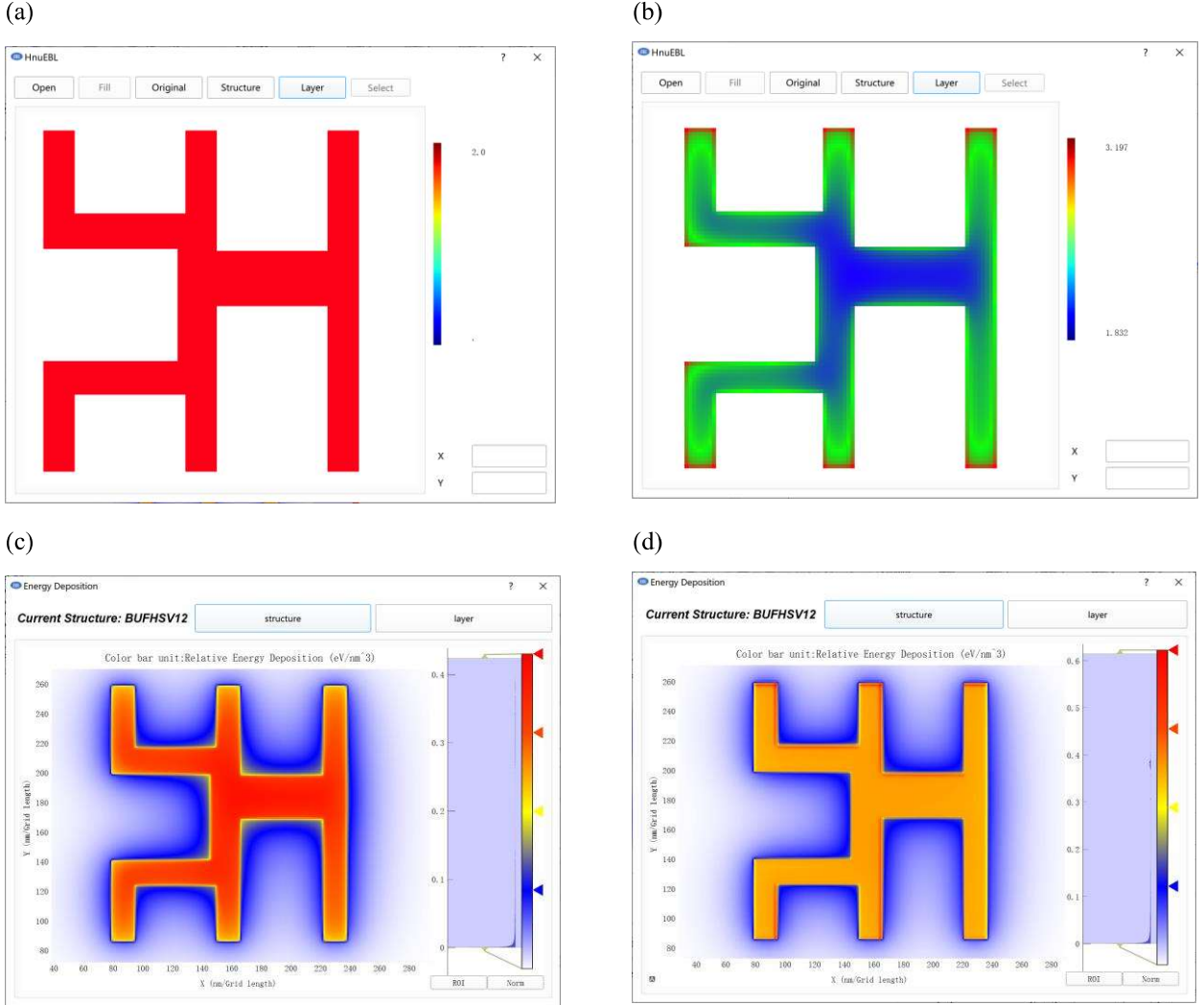


Fig. 3. Dose comparison before (a) and after (b) PEC in the GDSII file visualization module; energy deposition comparison before (c) and after (d) PEC.

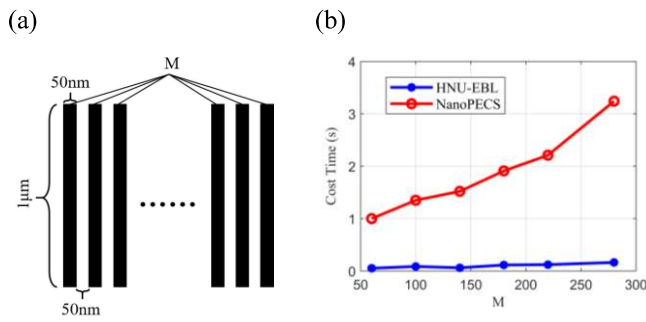


Fig. 4. (a) Schematic of the test layout that is M gratings with a size of $1\mu\text{m}\times 50\text{nm}$. (b) Comparison between the cost time of the proximity effect correction (PEC) in the HNU-EBL and NanoPECS.

IV. EBL QUALITY EVALUATION AND VISUALIZATION

The result of the difference between the placement of exposed layout (the inner edge of Fig. 5) and the original layout (the outer edge of Fig. 5) is called Edge Placement Error (EPE) [9]. In the EPE module (#6 in Fig. 1), before starting the EPE calculation, user should enter the PSF results, select a GDSII file, etc. The smaller the EPE value, the closer the exposed layout is to the original layout.

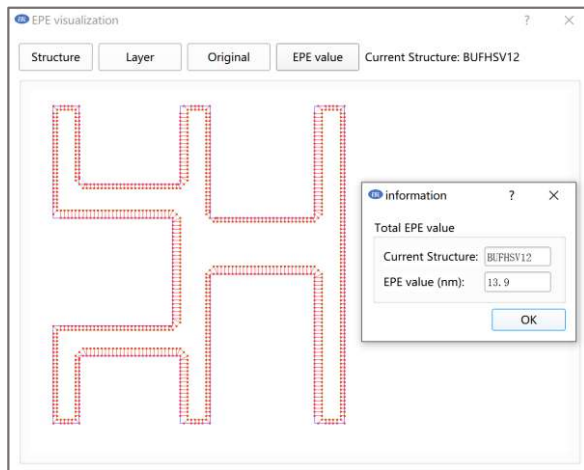


Fig. 5. EPE diagram of the layout and the interface of EPE value in HNU-EBL.

V. CONCLUSION

This paper presents a software toolkit (HNU-EBL) for EBL simulation and optimization to guide the experiments of researchers. It can calculate the trajectory and energy deposition of the electron beam under different parameters. And it performs PEC efficiently through several fitted PSF models. In addition, this toolkit also provides EPE auxiliary analysis and visualization of layout in GDSII format.

ACKNOWLEDGMENT

This work is supported by the National Natural Science Foundation of China (#61804049); the Fundamental Research Funds for the Central Universities of P.R. China; Huxiang High Level Talent Gathering Project (#2019RS1023); the Key Research and Development Project of Hunan Province, P.R. China (#2019GK2071); the Technology Innovation and Entrepreneurship Funds of Hunan Province, P.R. China (#2019GK5029); the Fund for Distinguished Young Scholars

of Changsha (#kq1905012); and the China Postdoctoral Science Foundation (#2020M682552).

REFERENCES

- [1] J. Zheng, J. Zhou, P. Zeng, Y. Liu, Y. Shen, W. Yao, et al., "30 GHz surface acoustic wave transducers with extremely high mass sensitivity," *Applied Physics Letters*, vol. 116, p. 123502, 2020.
- [2] J. Samà, G. Domènech-Gil, I. Gracia, X. Borriscé, C. Cané, S. Barth, et al., "Electron beam lithography for contacting single nanowires on non-flat suspended substrates," *Sensors and Actuators B: Chemical*, vol. 286, pp. 616-623, 2019.
- [3] Y. Xin, G. Pandraud, Y. Zhang, and P. French, "Single-Mode Tapered Vertical SU-8 Waveguide Fabricated by E-Beam Lithography for Analyte Sensing," *Sensors*, vol. 19, p. 3383, 2019.
- [4] J. Pavkovich, "Proximity effect correction calculations by the integral equation approximate solution method," *Journal of Vacuum Science & Technology B*, vol. 4, pp. 159-163, 1986.
- [5] M. Parikh, "Self-consistent proximity effect correction technique for resist exposure (SPECTRE)," *Journal of vacuum science and technology*, vol. 15, pp. 931-933, 1978.
- [6] P. Hudek, U. Denker, D. Beyer, N. Belic, and H. Eisenmann, "Fogging effect correction method in high-resolution electron beam lithography," *Microelectronic engineering*, vol. 84, pp. 814-817, 2007.
- [7] M. Ogasawara, N. Shimomura, J. Takamatsu, S. Yoshitake, K. Ooki, N. Nakayama, et al., "Reduction of long range fogging effect in a high acceleration voltage electron beam mask writing system," *Journal of Vacuum Science & Technology B: Microelectronics and Nanometer Structures Processing, Measurement, and Phenomena*, vol. 17, pp. 2936-2939, 1999.
- [8] T. Chang, "Proximity effect in electron-beam lithography," *Journal of vacuum science and technology*, vol. 12, pp. 1271-1275, 1975.
- [9] S. Banerjee, P. Elakkumanan, L. W. Liebmann, J. A. Culp, and M. Orshansky, "Electrically driven optical proximity correction," *Proceedings of SPIE - The International Society for Optical Engineering*, 2008.
- [10] M. Dapor, "Monte Carlo simulation of the interaction of electrons with supported and unsupported thin films," *Nuclear Instruments and Methods in Physics Research Section B: Beam Interactions with Materials and Atoms*, vol. 202, pp. 155-160, 2003.
- [11] M. Blytt, M. Kachelrieß, and S. Ostapchenko, "ELMAG 3.01: A three-dimensional Monte Carlo simulation of electromagnetic cascades on the extragalactic background light and in magnetic fields," *Computer Physics Communications*, vol. 252, 2020.
- [12] S. J. Wind, M. G. Rosenfield, G. Pepper, W. W. Molzen, and P. D. Gerber, "Proximity correction for electron beam lithography using a three-Gaussian model of the electron energy distribution," *Journal of vacuum science & technology. B, Microelectronics and nanometer structures: processing, measurement, and phenomena: an official journal of the American Vacuum Society*, vol. 7, pp. 1507-1512, 1989.
- [13] Raith GmbH, NanoPECS Software Description, Raith GmbH, 2008.
- [14] T. A. Fretwell, R. Gurung, and P. L. Jones, "Curve fitting to Monte Carlo data for the determination of proximity effect correction parameters," *Microelectronic Engineering*, vol. 17, pp. 389-394, 1992.
- [15] C. Hou, W. Yao, W. Liu, Y. Chen, and J. Liu, "Ultrafast and Accurate Proximity Effect Correction of Large-Scale Electron Beam Lithography based on FMM and SaaS," in *2020 International Workshop on Advanced Patterning Solutions (IWAPS)*, 2020.
- [16] M. Frigo and S. G. Johnson, "The design and implementation of FFTW3," *Proceedings of the IEEE*, vol. 93, pp. 216-231, 2005.
- [17] M. E. Haslam, "Two-dimensional Haar thinning for data base compaction in Fourier proximity correction for electron beam lithography," *Journal of Vacuum Science & Technology B: Microelectronics and Nanometer Structures*, vol. 3, 1985.
- [18] J. M. Pavkovich, "Proximity effect correction calculations by the integral equation approximate solution method," *Journal of Vacuum Science & Technology B: Microelectronics and Nanometer Structures*, vol. 4, 1986.